Patient-specific acetabular shape modelling: comparison among sphere, ellipsoid and conchoid parameterisations

Pietro Cerveri[a]*, Alfonso Manzotti[b] and Guido Baroni[a]

[a]*Dipartimento di Bioingegneria – Politecnico di Milano, via Golgi 39, I-20133 Milano, Italy;* [b]*Ist Orthopaedic Department, C.T.O. Hospital, Istituti Clinici di Perfezionamento, Milano, Italy*

(*Received 1 February 2012; final version received 11 June 2012*)

1. Introduction

The morphological coupling between the pelvic bone and the femur, and the constraints induced by cartilages, muscles and ligaments determine the hip joint kinematics and the load transfer from the acetabulum to the femoral head. Geometrically, the spherical-like aspect of the femoral head and the hemi-spherical-like aspect of acetabular cup support the assumption that the hip joint can be modelled, from a kinematic perspective, as a pure ball-and-socket joint. Nominally, this yields to consider three independent rotations of the femoral head, with respect to the acetabular cup, about a virtual pivot point, namely the hip joint centre (HJC) located in the geometrical centre of the femoral head.

In the domain of total hip arthroplasty (THA), accurate and repeatable pre-operative assessments of the HJC, on images and 3D models, and intra-operative, using either predictive (Bell et al. 1990; Piazza et al. 2004; Cereatti et al. 2007) or functional (Camomilla et al. 2006; Siston and Delp 2006; De Momi et al. 2009; Lenaerts et al. 2009; Heller et al. 2011) approaches, were a matter of intensive investigations. However, less interest was put on the validation of the sphericity assumption taking into account the osseous anatomy of the femoral head and the acetabulum.

The spherical coupling drove from the origin the prosthetic design of the acetabular and the head femoral components (Saikko and Calonius 2002; Pramanik et al. 2005). In the planning stage, the sphericity assumption allowed to quantify the implant size by using planar circular-shaped templates super imposed on the physical X-ray or by adopting digital spherical shapes using either CT images or 3D surface models. In the surgical phase, the ball-and-socket joint model allowed to apply functional methods based on pivoting movements of the leg to determine the idealised HJC.

Early anthropometric studies (Blowers et al. 1972; Bell et al. 1990; Menschik 1997; Shepherd and Seedhom 1999) showed that both the femoral head and the acetabular cup are rarely perfect spheres. The spherical coupling was also reported to be insufficient for the aim of understanding and taking care of different degenerative hip diseases (Ganz et al. 2003; Beck et al. 2005; Imam and Khanduja 2011; Urban et al. 2011). In addition, the intrinsic morphological variability, the degenerative effects of ageing

*Corresponding author. Email: pietro.cerveri@polimi.it

and the pathological conditions can make any single a priori model insufficient in accurately describing the morphologies of the two bony regions (Govsa et al. 2005; Köhnlein et al. 2009; Anderson et al. 2010; Nakahara et al. 2011), thus claiming for subject-specific shape analysis. A recent kinematic study, carried out on small cadaveric samples (four specimens), reported favourable results of ball-and-socket joint model whereas the authors acknowl-edged that the acetabular shape could be better modelled with geometries other than the sphere (Cereatti et al. 2010). The low number of the evaluation data-sets used in that study reduced the potential of the outcome.

Different parameterisations of the acetabular shape and the femoral head (rotational ellipsoids and conchoids) were studied aiming at improving the accuracy of HJC location for surgical planning purposes (Menschik 1997; Xi et al. 2003; Gu et al. 2008; Kang et al. 2011). In 1997, Menschik carried out a study on a small cadaveric data-set (eight specimens) and found that the conchoid shape was better representative for the femoral head, claiming that the conchoid-based joint could make the hip joint less likely to sublux than a ball-and-socket joint. The elliptical shape, used to represent acetabular cup, was hypothesised to reduce the risk of subluxation (Xi et al. 2003). On a data-set of 25 cadaveric specimens (Chinese race), it was shown that the rotational ellipsoid fitted the acetabular cup better than the theoretical spherical shape (Gu et al. 2008), resulting in less wear during bone motion. A more recent study, carried out on a MRI data-set acquired from 14 young healthy subjects, reinforced the value of the conchoid fitting with respect to the sphere (Kang et al. 2011).

In light of these premises, the purpose of this study was to analyse the morphology of the acetabular cup shape by comparing three different parameterisations, namely the sphere, the ellipsoid and the revolute conchoid shapes. Three-dimensional surface models, reconstructed from CT scans of cadavers and patients, were used to evaluate the potential shape variability. We carried out two concurrent analyses on:

(A) the overall cup shape including both the acetabular fossa and the lunate surface (geometrically consistent as the artificial cup would replace the overall acetabulum);
(B) the cup represented by the lunate surface only (physiologically consistent as the motion of the femoral head performs about this surface).

2. Materials and methods

2.1 Data collection

Eleven embalmed cadavers (nine males and two females of Caucasian race) with an average age of about 77 years (61–95) went through CT axial acquisition. Siemens Somatom Sensation 64 (Siemens AG, Erlangen, Germany) scanner, with a field of view of 38 by 38 cm, set to 140 kV and 48 mAs was used. About 650 contiguous axial slices (512 by 512 pixels) were taken at 1 mm scan interval from the upper pelvis to the proximal tibia. As two subjects underwent a THA on left and right hip, respectively, just 10 left and 10 right image data-sets were processed. No specimen showed sensible cartilage or bone defects in the hip joint. For each specimen, the 3D model of the outer surfaces of the two pelvic bones was created using Mimics (Materialise NV, Leuven, Belgium) application. Image segmentation was done through manual editing by radiological experts who separated the femoral head part and excluded the hip articular cartilage. In some cases, extra manual editing was needed to close the undue holes. In order to smooth the surface, 3D morphological opening was applied. A total of 20 hemi-pelvic bone surfaces were attained.

Eighteen additional hemi-pelvic bone surfaces were reconstructed from the CT scans (Siemens AG) of nine patients (six males and three females of Caucasian race), with an average age of about 59 years (28–91). Contiguous axial slices (512 by 512 pixels) were taken (scanning interval: 3 mm) from the upper pelvis to the proximal femur. The patients were investigated for potential cartilage damage at the hip joints. They were all diagnosed with early osteoarthritis. No bony damages were, however, detected in the images. The management, the anonymisation and the processing of the data-sets were approved by the Human Subject Committee of the C.T.O. Hospital in Milano, Italy. For each patient study, the outer surface of the pelvic bone was reconstructed using Amira software package (Visage Imaging GmbH, Berlin, Germany). The image segmentation was done through manual editing by one radiological expert who separated the femoral head part and excluded the hip articular cartilage. Early osteoarthritis conditions and lack of bone damages in all the patients allowed us to join the two data-sets in a single study group.

2.2 Surface models and data fitting

The overall acetabular region was obtained by automatic 3D segmentation (Figure 1) of the hemi-pelvic bone surfaces according to the methodology reported in Cerveri et al. (2011). The mean-shifted curvatures are computed on every vertex of the hemi-pelvic bone surface. Pit and ridge regions are detected using automatic thresholding. The vertices of the mesh are clustered into various regions on the basis of the two curvature descriptors. After processing the clusters in the pit region, one single cluster for the internal shape of the acetabulum is obtained. The clusters belonging to ridge regions are processed to obtain one single consistent cluster for the acetabular rim. The two regions are merged into a single surface representative of the acetabular cup. The lunate surface was extracted

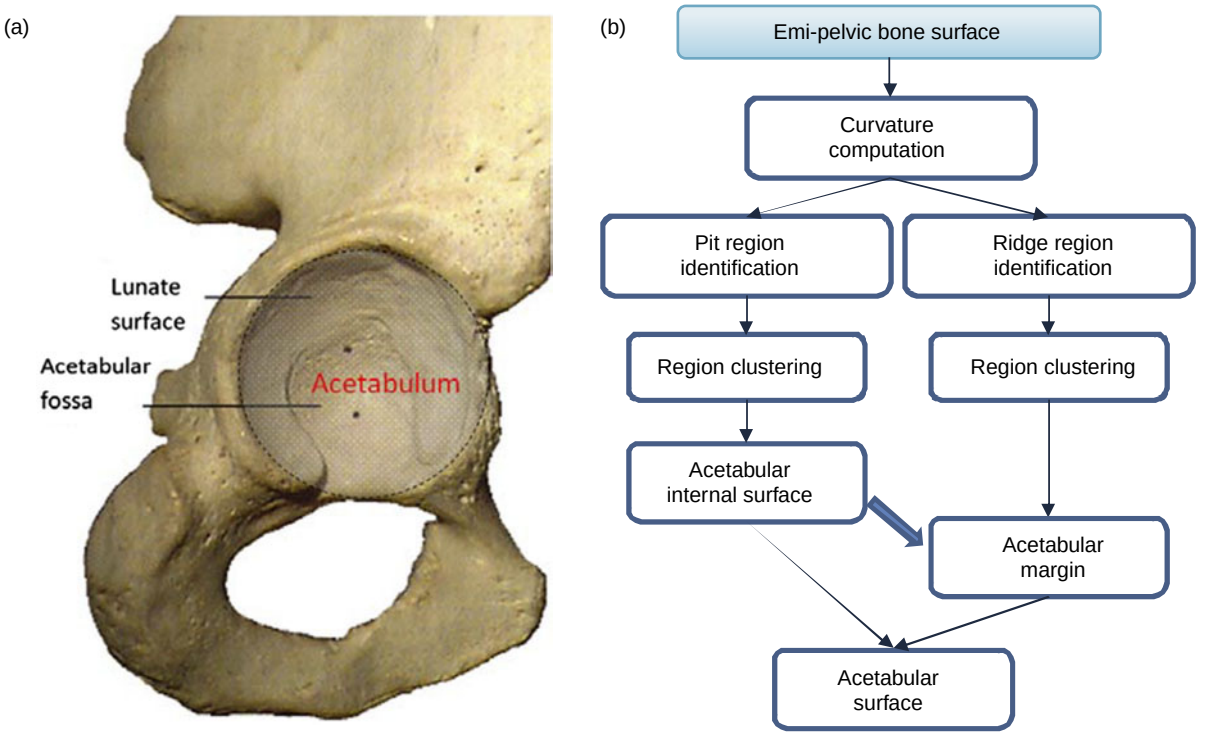

Figure 1. (a) Morphological detail of the acetabulum in the pelvic bone: the acetabular surface is separated by the acetabular fossa and lunate surface; (b) general schema of the acetabular cup segmentation (Cerveri et al. 2011).

from each acetabular shape by a manual cutting of the acetabular fossa in the Amira software.

Three different parameterisations, namely the sphere, the ellipsoid and the revolute conchoid shapes, were taken into account. Considering the sphere radius r and the centre $C(xo, yo, zo)$, the Cartesian sphere equation is

$$(x - xo)^2 + (y - yo)^2 + (z - zo)^2 = r^2. \quad (1)$$

A nonlinear least square fitting based on Levenberg–Marquardt strategy with explicit Jacobian computation was used to compute the optimal sphere parameters.

For the ellipsoid, the following equation can be written as

$$\frac{(x - xo)^2}{a^2} + \frac{(y - yo)^2}{b^2} + \frac{(z - zo)^2}{c^2} + mxy + nxz + lyz + k = 0 \quad (2)$$

which considers the ellipsoid form factors (a, b, c) and the translation and the orientation. Similar to the sphere fitting case, a nonlinear least square fitting based on Levenberg–Marquardt strategy was used. The acetabular axis, computed according to Cerveri et al. (2011), provided the initial value of the major axis of the ellipsoid.

The conchoid curve is described in polar coordinates by the following equation

$$r = b + a\cos(v), \quad (3)$$

where r is a curve with length measured from the centre of the conchoid (O), a and b are the form factors and v is the angle between curve r and the y-axis (Figure 2(a)). Equation (3) represents actually the Limaçon of Pascal, which is a conchoid of a circle with respect to the circle origin, O. In order to preserve uniformity with former studies (Menschik 1997; Xi et al. 2003; Kang 2011), this curve is referred to as a conchoid herein.

Let $(x^2 + y^2 - ax)^2 = b^2(x^2 + y^2)$ be the Cartesian representation of conchoid curve; the corresponding conchoid shape in the canonical form is obtained by revoluting the curve about the X-axis as

$$(x^2 + y^2 + z^2 - ax)^2 = b^2(x^2 + y^2 + z^2) \quad (4)$$

which is a fourth-order surface like the torus. Dealing explicitly with the translation and the rotation with respect to the canonical form is not straightforward and can increase the complexity of the fitting problem. Alternatively, we adopted an indirect method, however automatic, to the estimation of the translated and rotated revolute conchoid based on an evolutionary approach, namely the evolution strategy $(1, \lambda)$ with covariance matrix adaptation (Cerveri et al. 2001). The idea was to rigidly transform the acetabular cup surface and to estimate the form factors of the revolute conchoid in its canonical form a posteriori iteratively minimising the fitting error.

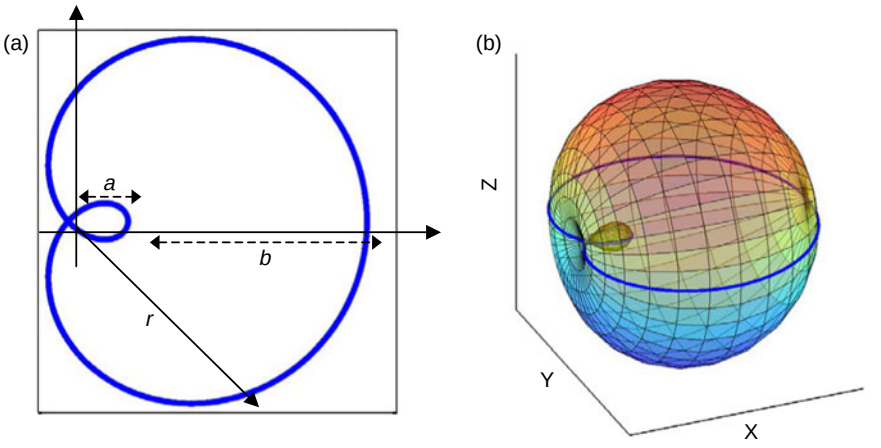

Figure 2. (a) A conchoid curve with general equation $r = b + a\cos(v)$. (b) The corresponding 3D rotational shape.

The optimisation problem was therefore reframed into the estimation of eight parameters, explicitly the two form factors a and b of the conchoid (see Equation (4)), and the three translation coordinates and the three orientation angles which account for the rigid transform of the cup. After aligning the main axis of the cup with the X-axis, according to the estimated acetabular axis (Cerveri et al. 2011), and the cup posterior margin with the posterior margin of the conchoid shape, the procedure generated an initial random guess (new population: $\lambda = 25$) of the parameters through the mutation function. According to the value of the radius r_s of the fitted sphere, the initial values of a and b were randomly generated starting by r_s and $0.5r_s$, respectively. The fitting error, the surface distance between the cup and the conchoid, was then computed by sampling the conchoid surface. At each iteration step, the best element (lowest fitting error) in the population was selected to be the father for the next epoch. If the form factors are consistent with the Limaçon of Pascal shape ($|a| > |b|$), the rigid transform was applied to the acetabular cup surface. The mutation function, adapted according to the results of the selection, drove the generation of more and more reliable solutions. The evolutionary optimisation stopped when the step size of the mutation function was under a predefined ($1e-5$) threshold t (Figure 3).

2.3 *Data analysis*

The fitting errors of the cadaveric and patient data-sets were compared across the three parameterisations in terms of median value (lower and upper quartiles). Both the overall acetabulum (case A) and the lunate surface only (case B) were considered. For each case, the statistical analysis of the results was carried out using a one-way analysis of variance done through the non-parametric Kruskall–Wallis test (Matlab, Matworks, Inc., Natick, MA, USA). A multiple comparison (*post hoc*) procedure was used to strictly determine which pairs of mean ranks were significantly different and which were not. A statistically significant result was given a p value <0.05. The statistical difference between the two cases A and B was also analysed.

The consistency of the fitted ellipsoid and conchoid shapes to the acetabular geometry was determined by

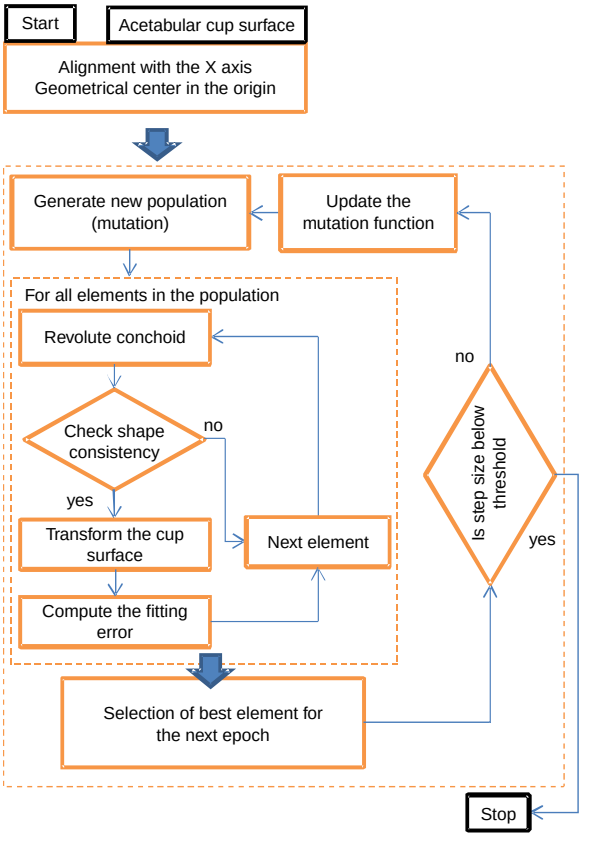

Figure 3. The flowchart of the algorithm (1, λ)-ES for estimating the parameters of the revolute conchoid shape.

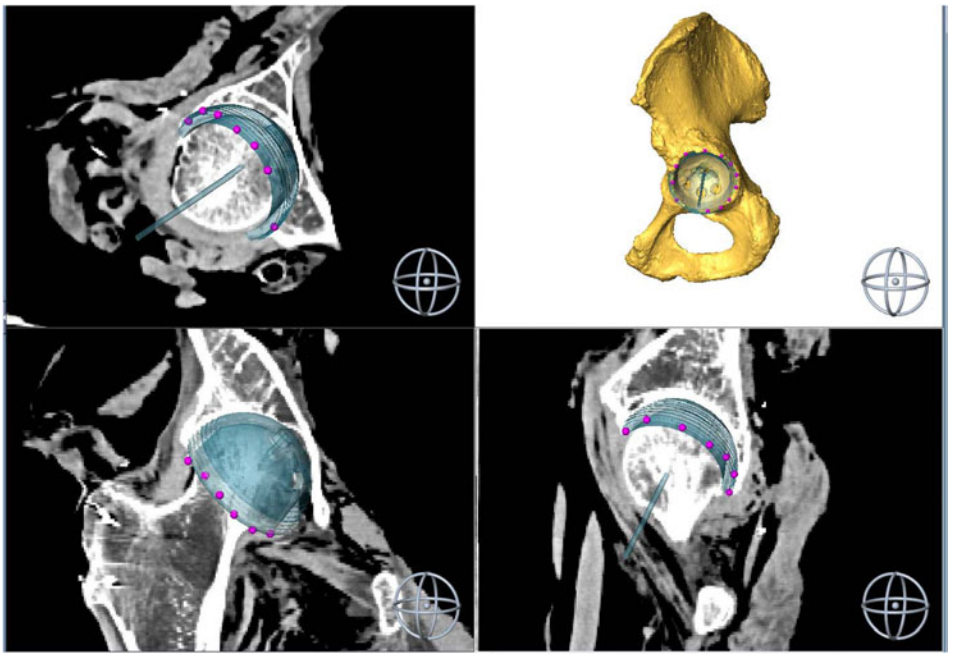

Figure 4. Template (artificial acetabular cup along with a stick orthogonal to the cup plane) utilised in AMIRA package to manually determine the acetabular axis.

comparing the principal axis of the shapes with the acetabular axis obtained by manual detection. One expert in radiological orthopaedic imaging, with advanced skills in 3D computer-aided surgical planning, performed the axis identification in the Amira software package directly on the bone models locating a set of 12 landmarks, approximately uniformly spaced, on the acetabular rim. Such landmarks defined the acetabular plane, the normal direction of which is just the acetabular axis, and therefore the normal direction of the cup (Figure 4). The operator manually scaled and arranged the position of the virtual cup model to fit the acetabular surface. The operator was free to cross-check the axis on the original CT axial images and interact with the artificial cup model to further refine it. The angular error between the manual acetabular axis and the main axis of the ellipsoid and conchoid shapes was computed for each surface model. The root mean squared error of the overall angular error distribution was obtained.

3. Results

The boxplot of the error distributions for case A showed that the median fitting errors of both the ellipsoid (1.14 mm) and the conchoid (1.28 mm) fitting are lower than the fitting errors obtained through the sphere (1.95 mm) fitting (Figure 5). The statistical comparison provided a very low global significance ($p < 1e-10$). The post hoc comparison yielded to a significance of the difference between ellipsoid and sphere ($p < 2.50e-10$) and between conchoid and sphere ($p < 1.07e-09$). No significant difference was found for the comparison between ellipsoid and conchoid ($p > 0.08$).

Analogously, the boxplot of the error distributions for case B showed that the median fitting errors of both the ellipsoid (0.99 mm) and the conchoid (1.18 mm) fitting are lower than the fitting errors obtained through the sphere (1.89 mm) fitting (Figure 6). Similar to the previous case, significance of the difference between ellipsoid and sphere

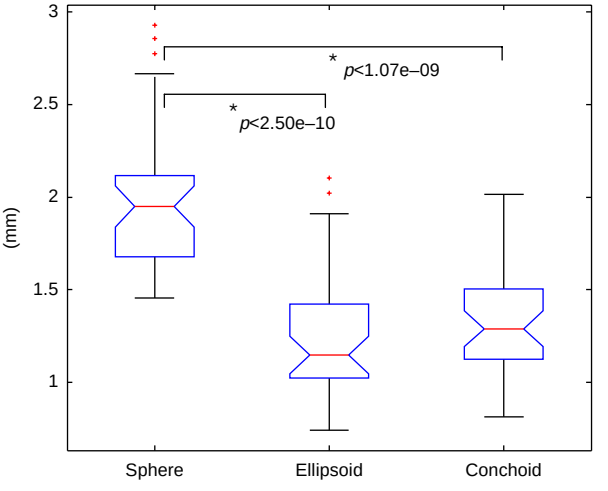

Figure 5. Boxplots of the results for case A (overall acetabular surface). On each box, the central mark is the median, the edges of the box are the 25th and 75th percentiles and the whiskers extend to the most extreme data points excluding outliers that are plotted individually as red crosses. Asterisk represents significant difference.

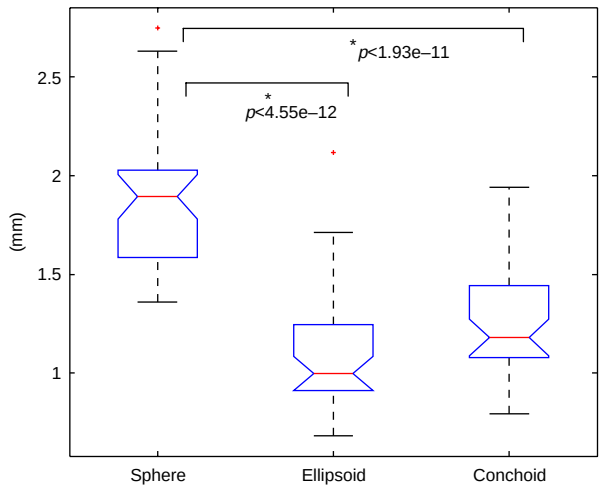

Figure 6. Boxplots of the results for case B (lunate surface). On each box, the central mark is the median, the edges of the box are the 25th and 75th percentiles and the whiskers extend to the most extreme data points excluding outliers that are plotted individually as red crosses. Asterisk represents significant difference.

($p < 4.55e-12$) and between conchoid and sphere ($p < 1.93e-11$) was found. Interestingly and differently from case A, case B provided significant difference in the fitting between ellipsoid and conchoid ($p < 0.01$).

The between-group comparison (A vs. B) showed that significance of the difference ($p < 0.02$) was detected for the ellipsoid fitting whereas no significance was found for both sphere and conchoid.

The median angular errors (Figure 7) between the principal shape axes of the ellipsoid and conchoid with respect to the manually measured acetabular axis were $<8°$ with maximal range (quartiles) lower than 3.5°. Specifically, for the case A they were 7.57° and 6.33°, respectively. The statistical difference was not significant ($p > 0.16$). For case B, the median errors decreased to 6.42° and 5.66°, respectively, with no statistical difference in between the two distributions ($p > 0.10$). The between-cases statistical difference was found to be not significant (Ellipsoid – case A vs. case B: $p > 0.13$; Conchoid – case A vs. case B: $p > 0.40$).

4. Discussion and conclusion

The human acetabular shape is commonly represented as a hemisphere, but there have been no extensive quantitative assessments of this assumption in the literature. Our aim was to contribute to the ongoing debate and to test the limits and validity of this hypothesis by comparing three different parameterisations, namely the sphere, the ellipsoid and the rotational conchoid. Similar to the conchoid shape (Menschik 1997), the ellipsoid shape was considered as it can constrain the movement of the hip joint in the coronal plane but does not influence the movement of a joint in the sagittal plane, thus improving the joint stability and decreasing the subluxation compared with a ball-and-socket joint. The rim of the acetabulum on the opening plan has been reported as ellipsoid with reduced anterior–posterior and increased inferior–superior axes (Eckstein et al. 1997). The fitted ellipsoid of the acetabulum is consistent with this conclusion, because the intersection of the ellipsoid and the plane on the acetabular rim is approximately an ellipse.

We analysed both the overall acetabulum, composed by the lunate surface and the acetabular fossa, and the acetabular part effectively devoted to the motion interface with the femoral head (lunate surface). This was motivated by the consideration that the potential prediction of the spatial distribution of the joint load should take into account just the contact interface between the two bony parts, namely the lunate surface of the acetabulum and the head of the femur.

The analysis was carried out on a data-set of hemi-pelvic bone surfaces reconstructed from CT imaging taken from

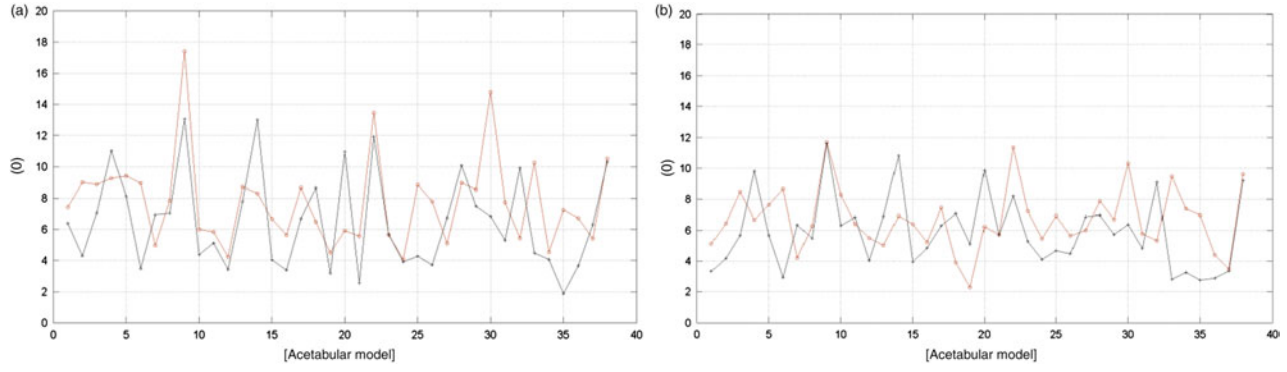

Figure 7. Angular errors between the principal shape axis (circle is for ellipsoid, cross is for conchoid) and the acetabular axis manually detected. (a) The median (case A) errors of the two distributions were 7.57° and 6.33° for the ellipsoid and the conchoid, respectively. The statistical difference was not significant ($p > 0.16$). (b) The median (case B) errors of the two distributions were 6.42° and 5.66° for the ellipsoid and the conchoid, respectively. The statistical difference was not significant ($p > 0.10$).

cadavers and patients. The diagnostic analysis, carried out on the patient group, evinced very little decrease of inter-osseous spaces, corresponding to reduced cartilage damages, and no bone defects at the hip joint. This condition was similar for the cadaver data-set, which allowed us to consider a single homogeneous group from the two data-sets.

Minor differences from the three idealised geometries were found (median range <1 mm). Nonetheless, the ellipsoid fitting was detected to be statistically different from the sphere fitting in agreement with Gu et al. (2008). Similarly, we found that the conchoid fitting was statistically different from the sphere fitting in agreement with Menschik (1997) and Kang et al. (2011). This was true for both case A and case B. The fitting comparison between ellipsoid and conchoid provided interesting results, showing that when considering the acetabular cup as composed by the lunate surface only (case B), the fitting quality of the ellipsoid is statistically better than that of the conchoid. From this result, we argue that the part of the acetabular fossa somewhat disrupts the fitting process on the overall acetabular cup and suggests that only the lunate surface should be considered for the parameterisation of the acetabular shape. Technically, this paper introduced some interesting innovations with respect to the literature about the same topic. Firstly, it exploited the algorithmic framework presented by the same author's group (Cerveri et al. 2011) to automatically extract the acetabular shape from the hemi-pelvic bone. This approach, which moves along the ongoing development of automatic methodologies for orthopaedic surgical planning (Otomaru et al. 2009; Weaver et al. 2009; Urban et al. 2011), was demonstrated to reduce the effect of the operator variability during the manual 3D segmentation. Secondly, the study was carried out on a significant number of acetabular shapes (38) taken from CT data-sets. Past studies on the same topic used less than 15 data-sets (Cereatti et al. 2010; Kang et al. 2011). Thirdly, the implemented fitting was fully automatic without any additional operator interaction overcoming the approach done by Kang et al. (2011), which was based on a manual-driven method to adjust the conchoid shape and location parameters on MRI images following the boundary curve of the acetabular rim profile. Fourthly, the comparison between the ellipsoid and the conchoid shapes was not previously reported. The advantage of considering both idealised geometries was that they can be used to obtain an estimation of the HJC, different from that of the sphere fitting centre, and from that of the acetabular axis, as well. This last quantity is known to be fundamental for the surgical planning and treatment of the THA. For instance, the ellipsoid and the conchoid can be used to predict the HJC in pre-operative planning of hip joint resurfacing operations, such as resections of non-spherical regions of the femoral head and neck junction in the treatment of early-stage degenerative hip disease to reduce impingement, and of hip joint prosthesis to decrease potential placement errors. Equivalently, such models can be an alternative to the classical sphere model in determining the mechanical axis of the lower limb, which is a critical landmark for total knee arthroplasty, both prior and following the surgery.

Finally, it evaluated the fitting quality of the two idealised geometries by comparing the alignment of the principal axis of the shapes to the acetabular axis manually identified on original CT images by a radiological expert. This was done to check that the increased fitting, potentially supported by more degrees of freedom in both models compared with the sphere, would be not corresponding to undue shape positioning incoherent with the principal direction of the acetabulum. The results showed that no statistical difference was found between the methods of determining axis alignments, supporting the conclusion that both model-based acetabular axes were consistent with the acetabular shape and mostly in accordance with expert knowledge (Figure 7). However, a bias and an absolute difference with regard to the manual measures of about $5°-7°$ and up to $16°$, respectively, were found. Although the margin of the acetabulum was considered a valid reference (Viceconti et al. 2003; Wong et al. 2010) for determining the acetabular axis (this was the method adopted in this work for the manual identification), the morphological variability and even little pathological conditions can modify the shape of the acetabular margin, thus disturbing the axis determination. The model-based method, adopted in this paper, can in principle reduce such effects as the axis determination is not just function of the margin but it depends on the overall shape. More extensive analyses would be needed, but are out of scope of this study.

A couple of potential drawbacks of this work can be summarised herewith. First, we neglected the role of the cartilage in determining the geometry of the acetabular shape differently from other previous studies (Kang et al. 2011). Although this simplification can lose the effect of the soft tissue interface between the femoral head and the acetabulum, it is reasonable assuming that the cartilage shape deforms in function of the loading condition, and its role in determining the geometry of the interface is less relevant (Anderson et al. 2010). Therefore, it appears that computing the HJC as the centre of the fitting conchoid to the hip joint cartilage could bias the estimation and lose the generality of the results. Second, we did not exploit the estimated geometries to predict the cartilage stress during dynamic conditions of loading as described in Anderson et al. (2010). We acknowledge that this could be a further validation of the approach, but, however, this was out of scope of this paper. Future developments, aiming at addressing this topic, will move towards the comparison among idealised and patient-specific morphologies.

In conclusion, we can synthesise that the osseous morphology of the acetabular cup can be parameterised

both with an ellipsoid shape and with a conchoid shape as well with superior quality than the simple sphere. Differently, if one considers just the lunate surface, better fitting results are expected when using the ellipsoid. In terms of HJC, pre-operative approaches to its estimation using either images or surface models should take into account that the spherical model can be inferior to other geometries as shown in this study.

References

Anderson AE, Ellis BJ, Maas SA, Weiss JA. 2010. Effects of idealized joint geometry on finite element predictions of cartilage contact stresses in the hip. J Biomech. 43(7): 1351–1357.

Bell AL, Petersen DR, Brand RA. 1990. A comparison of the accuracy of several hip center location prediction methods. J Biomech. 23:617–621.

Beck M, Kalhor M, Leunig M, Ganz R. 2005. Hip morphology influences the pattern of damage to the acetabular cartilage: femoroacetabular impingement as a cause of early osteoarthritis of the hip. J Bone Joint Surg Br. 87(7): 1012–1018.

Blowers DH, Elson R, Korley E. 1972. An investigation of the sphericity of the human femoral head. Med Biol Eng. 10: 762–775.

Camomilla V, Cereatti A, Vannozzi G, Cappozzo A. 2006. An optimized protocol for hip joint centre determination using the functional method. J Biomech. 39:1096–1106.

Cereatti A, Camomilla V, Vannozzi G, Cappozzo A. 2007. Propagation of the hip joint centre location error to the estimate of femur vs pelvis orientation using a constrained or an unconstrained approach. J Biomech. 40:1228–1234.

Cereatti A, Margheritini F, Donati M, Cappozzo A. 2010. Is the human acetabulofemoral joint spherical? J Bone Joint Surg Br. 92-B(2):311–314.

Cerveri P, Marchente M, Chemello C, Manzotti A, Confalonieri N, Baroni G. 2011. Advanced computational framework for the automatic analysis of the acetabular morphology from the pelvic bone surface for hip arthroplasty applications. Ann Biomed Eng. 39(11):2791–2806.

Cerveri P, Pedotti A, Borghese NA. 2001. Combined evolution strategies for dynamic calibration of video based measurement systems. IEEE Trans Evol Comput. 5(3):271–282.

De Momi E, Lopomo N, Cerveri P, Zaffagnini S, Safran MR, Ferrigno G. 2009. In-vitro experimental assessment of a new robust algorithm for hip joint centre estimation. J Biomech. 42(8):989–995.

Eckstein F, von Eisenhart-Rothe R, Landgraf J, Adam C, Loehe F, Müller-Gerbl M, Putz R, 1997. Quantitative analysis of incongruity, contact areas and cartilage thickness in the human hip joint. Acta Anat (Basel). 158:192–204.

Ganz R, Parvizi J, Beck M, Leunig M, Notzli H, Siebenrock KA. 2003. Femoroacetabular impingement: a cause for osteoarthritis of the hip. Clin Orthop Relat Res. 417:112–120.

Govsa F, Ozer MA, Ozgur Z. 2005. Morphologic features of the acetabulum. Arch Orthop Trauma Surg. 125(7):453–461.

Gu D, Chen Y, Dai K, Zhang S, Yuan J. 2008. The shape of the acetabular cartilage surface: a geometric morphometric study using three-dimensional scanning. Med Eng Phys. 30(8): 1024–1031.

Heller MO, Kratzenstein S, Ehrig RM, Wassilew G, Duda GN, Taylor WR. 2011. The weighted optimal common shape technique improves identification of the hip joint center of rotation in vivo. J Orthop Res. 29(10):1470–1475.

Imam S, Khanduja V. 2011. Current concepts in the diagnosis and management of femoroacetabular impingement. Int Orthop. 35(10):1427–1435.

Kang MJ, Sadri H, Stern R, Magnenat-Thalmann N, Hoffmeyer P, Ji HS. 2011. Determining the location of hip joint centre: application of a conchoid's shape to the acetabular cartilage surface of magnetic resonance images. Comput Methods Biomech Biomed Eng. 14(1):65–71.

Köhnlein W, Ganz R, Impellizzeri FM, Leunig M. 2009. Acetabular morphology: implications for joint-preserving surgery. Clin Orthop Relat Res. 467(3):682–691.

Lenaerts G, Bartels W, Gelaude F, Mulier M, Spaepen A, VanderPerre G, Jonkers I. 2009. Subject-specific hip geometry and hip joint centre location affects calculated contact forces at the hip during gait. J Biomech. 42: 1246–1251.

Menschik F. 1997. The hip joint as a conchoid shape. J Biomech. 30:971–973.

Nakahara I, Takao M, Sakai T, Nishii T, Yoshikawa H, Sugano N. 2011. Gender differences in 3D morphology and bony impingement of human hips. J Orthop Res. 29(3):333–339.

Otomaru I, Kobayashi K, Okada T, Nakamoto M, Kagiyama Y, Takao M, Sugano N, Tada Y, Sato Y. 2009. Expertise modeling for automated planning of acetabular cup in total hip arthroplasty using combined bone and implant statistical atlases. Med Image Comput Comput Assist Interv. 12(Pt 1): 532–539.

Piazza SJ, Erdemir A, Okita N, Cavanagh PR. 2004. Assessment of the functional method of hip joint center location to reduced range of hip motion. J Biomech. 37:349–356.

Pramanik S, Agarwal AK, Rai KN. 2005. Chronology of total hip joint replacement and materials development. Trends Biomater Artif Organs. 19(1):15–26.

Saikko V, Calonius O. 2002. Slide track analysis of the relative motion between femoral head and acetabular cup in walking and in hip simulators. J Biomech. 35:455–464.

Shepherd DE, Seedhom BB. 1999. Thickness of human articular cartilage in joints of the lower limb. Ann Rheum Dis. 58(1): 27–34.

Siston RA, Delp SL. 2006. Evaluation of a new algorithm to determine the hip joint center. J Biomech. 39:125–130.

Urban JE, Weaver AA, Theivendran K, Stitzel JD. 2011. Acetabular rim profile measurement in femoroacetabular impingement patients. Biomed Sci Instrum. 47:118–123.

Viceconti M, Lattanzi R, Antonietti B, Paderni S, Olmi R, Sudanese A, Toni A. 2003. CT-based surgical planning software improves the accuracy of total hip replacement preoperative planning. Med Eng Phys. 25:371–377.

Weaver AA, Gilmartin TD, Anz AW, Stubbs AJ, Stitzel JD. 2009. A method to measure acetabular metrics from three dimensional computed tomography pelvis reconstructions. Biomed Sci Instrum. 45:155–160.

Wong KC, Kumta SM, Leung KS, Ng KW, Ng EWK, Lee KS. 2010. Integration of CAD/CAM planning into computer assisted orthopaedic surgery. Comput Aided Surg. 15(4–6): 65–74.

Xi J, Hu X, Jin Y. 2003. Shape analysis and parameterized modeling of hip joint. J Comput Inform Sci Eng. 3(3): 260–265.